

High GNG13 expression is associated with poor survival in epithelial ovarian cancer and breast cancer

Yuanlin LIU^{1,2*}, Shuting GU^{2*}, Tong WU^{3*}, Yunzhao XU², Qi MENG², Zongyu GUAN², Xiaojing ZHANG⁴, Xiaoli SUN², Yi SHEN⁵, Haowen FAN⁶, Changjiang GU^{2*}, Jinlian FENG^{7*}

¹Department of Obstetrics and Gynecology, Shanghai First Maternity and Infant Health Hospital, Shanghai, China; ²Department of Obstetrics and Gynecology, Affiliated Hospital of Nantong University, Nantong, Jiangsu, China; ³Department of Gastroenterology, Affiliated Hospital and Medical School of Nantong University, Nantong, Jiangsu, China; ⁴Department of Clinical Biobank, Affiliated Hospital of Nantong University, Nantong, Jiangsu, China; ⁵Department of Epidemiology and Health Statistics, Nantong University, Nantong, Jiangsu, China; ⁶Department of Clinical Medicine, School of Medicine, Nantong University, Nantong, Jiangsu, China; ⁷Department of Obstetrics and Gynecology, Nantong Geriatric Rehabilitation Hospital, Nantong, Jiangsu, China

*Correspondence: cherubimliu@126.com; changjiang058@yeah.net

*Contributed equally to this work.

Received June 3, 2021 / Accepted July 15, 2021

Recently, change in the GNG13 expression has been shown to result in multiple congenital malformations and sexual reversal, and it was also found in the brain. The aim of this study was to measure the expression levels in epithelial ovarian cancer (EOC) and breast cancer (BC) and assess their value as a potential prognostic marker. The correlation of GNG13 protein expression was detected by immunohistochemistry (IHC) in 119 EOC and 125 BC tissues. Assessment of the associations between GNG13 levels and various clinicopathological features was identified, the relationship between GNG13 and prognosis in BC and EOC patients was analyzed using online resources of OncoPrint and Kaplan-Meier plotter. Protein expression levels of GNG13 were both significantly lower in BC and EOC compared with normal tissues ($p < 0.0001$ and $p < 0.001$, respectively). Among the clinicopathological characteristics of BC, tumor grade ($p = 0.001$) and TNM stage ($p = 0.001$) were significantly associated with low expression of GNG13. While in EOC, low expression of GNG13 was significantly related to FIGO stage ($p = 0.001$), presence of metastasis ($p = 0.001$), and CA125 ($p = 0.001$). Our data suggest that GNG13 expression maybe as a new inhibitor, which can strongly inhibit metastasis and partially attenuates tumor growth in EOC and BC.

Key words: guanine nucleotide-binding protein 13, breast cancer, epithelial ovarian cancer, prognosis, poor survival

Understanding of breast and ovarian cancers has greatly increased over recent decades [1, 2]. Ovarian cancer causes the greatest number of cancer deaths among women aged 50–70 years in China, and other countries [3]. In the past 30 years, 30% of patients with EOC live 5 years after their diagnoses [4]. Breast cancer (BC) has the highest morbidity and mortality of diagnosed cancers among women worldwide [5–7] but is a heterogeneous disease influenced by natural history, and environmental, genetic, behavioral, and other factors [8]. Two diseases share some risks, including diet and hormonal factors [9]. The Cancer Genome Atlas (TCGA) [7] also indicates strong gene-based similarities between BC and EOC. The discovery of BRCA1 and BRCA2 genes and their associations with BC and EOC [10, 11] prompted changes in our understanding of genetic factors

in the etiology of common cancers, but only 8–10% of the diseases are caused by BRCA1/2 mutations [12, 13]. Other genome-based risk elements are likely to be identified, and their associated proteins may provide new biomarkers to diagnose and monitor BC and EOC.

Guanine nucleotide-binding protein-13 γ (GNG13) [14], is encoded by the GNG13 gene and is mainly expressed in the ovary [15] and belongs to the guanine nucleotide-binding protein (G-protein) subunit [16]. Fujino et al. [17] found that GNG13 expression is limited to gonads during ovarian differentiation. Erickson et al. [15] found that GNG13 expression can be altered, resulting in multiple congenital malformations and sexual reversal. GNG13 has also been found in brain tissue, taste receptor cells [16], olfactory epithelium and retinal ON bipolar cells, and early-developing ovary. It

is reportedly expressed in retinal and neuronal tissues and plays an especially critical role in taste signal transduction [18]. However, the role of GNG13 in tumor tissues has not been widely studied.

As patients with EOC or BC are typically diagnosed at advanced stages with few early warning symptoms, they tend to have poor prognoses. A reliable biomarker for early-stage disease is therefore urgently needed. We hypothesized that GNG13 expression could be a marker for EOC and BC. Our study used tissue microarray immunohistochemistry (TMA-IHC) to evaluate both diseases. We then analyzed the relationship between GNG13 expression and various clinicopathological features in EOC and BC. Our findings were supported by bioinformatics analysis, the Oncomine and Kaplan-Meier plotter databases.

Patients and methods

Analysis of GNG13 expression in epithelial ovarian cancer and breast cancer. To verify GNG13 expression in GC, we explored the expression of GNG13 mRNA in the Oncomine database (<https://www.oncomine.org>).

Patients and tissue samples – ovarian cancer. We collected specimens from 213 patients who underwent surgery for EOC at the Gynecology Department of the Affiliated Hospital of Nantong University. These tissues were embedded in paraffin while fixed with formalin. All patients underwent standardized surgery and/or chemotherapy for at least 6 cycles after resection. Of the specimens, 119 were ovarian carcinoma (84 serous carcinomas, 18 endometrioid tumors, and 17 other types); 77 showed stage I–II diseases and 42 showed stage III–IV diseases; 91 were histologically high-grade tumors and 28 were low-grade, based on the International Federation of Obstetrics and Gynecology (FIGO) criteria.

Patients and tissue samples – breast cancer. All the patients had undergone mastectomy and/or axillary dissection (radical or functional, based on clinical and surgical findings). None of the patients received preoperative radiotherapy or chemotherapy before surgery. Postoperative histological examination confirmed lymph node metastasis in all patients. The initial clinical data were collected simultaneously from the hospital's medical records, including tumor grade, hormone receptor (ER/PR) status, patient age, tumor size, ERB-B2 receptor tyrosine kinase 2 (HER2) expression, Ki-67 status, triple-negative BC (TNBC) status (i.e., PR–/ER–/HER2– tumors), lymph node metastasis and TNM stage [19]. Tissues for the TMA were formalin-fixed and paraffin-embedded and had been obtained between 2005 and 2015. The TMA was made by Tissue Microarray System (Quick-Ray, UT06, UNITMA, Korea).

The study obtained the permission of the Human Research Ethics Committee of the Affiliated Hospital of Nantong University, Jiangsu, China. The study was approved by the Ethics Committee of the Affiliated Hospital of Nantong

University and all experiments were performed in accordance with approved guidelines of the Affiliated Hospital of Nantong University.

RNA extraction and qRT-PCR. RNAs from GIST, gastric and intestinal cancer tissues were prepared using TRIzol reagent (Invitrogen, Karlsruhe, Germany) in accordance with the manufacturer's instructions. Primers, RNA extraction, and qRT-PCR procedures are published. Primer sequences were as follows [20]: GNG13: forward 5'-CTGCTTTT-GCTGTCTCCTCC-3' and reverse 5'-AGGCCAGTTG-GTACTTGAGG-3' [21]. GAPDH: forward 5'-AGAAGGCTGGGGCTCATTG-3' and reverse 5'-AGGGGCCATC-CACAGTCTTC-3'.

Western blotting. Radioimmunoprecipitation (RIPA) lysis buffer containing PMSF was used to extract the cell sample protein, of which the experimental procedure was performed as described previously [22]. The rabbit anti-human GNG13 (Signalway antibody, #46004, 1:200), anti-CEMIP (cell migration-inducing protein, 1:1000, Abclonal, Woburn, MA, USA), p-STAT3 (Cell signaling Technology, #9145, 1:2000), STAT3 (Santa Cruz, sc-8019, 1:1000) polyclonal antibody were used as primary antibodies. The PVDF membranes were incubated with the HRP-conjugated goat anti-rabbit IgG as the secondary antibody (Proteintech, SA00001-1, SA00001-2, 1:5000). Results were analyzed using ImageJ 2X software (NIH, Bethesda, MD, USA).

Immunohistochemistry. The IHC methods were performed as previously described [22]. All tissue samples were fixed in 10% buffered formalin solution overnight and embedded in paraffin at room temperature. Paraffin-embedded (5 μ m) sections were divided into core tissue biopsies (2 mm in diameter) to make TMA. Sections were deparaffinized and then incubated with 3% H₂O₂, which was methanol for 15 min to quench endogenous peroxidase. Sections were then incubated with primary goat anti-GNG13 antibody (No. NBP1-91950, 1:200; Novus Biologicals, USA) overnight at 4°C. After washing with phosphate-buffered saline, sections were incubated with horseradish peroxidase-conjugated donkey anti-goat antibody (Abcam) for 15 min and then washed again.

Two investigators used an Olympus BX53 microscope (Olympus Co, Tokyo, Japan) to quantify GNG13 immunostaining, by scoring staining intensity as 0 (–, no staining), 1 (+, mild staining), 2 (++, medium staining), or 3 (+++, intense staining) and percentages of cells that stained positive.

We used the X-tile software program (The Rimm Lab at Yale University; <http://www.tissuearray.org/rimmlab>) to identify the optimal cut-off point for GNG13 IHC scores in terms of patients' overall survival (OS). We used the cut-off 120; 0–120 was considered low expression and 121–300 was high expression.

Statistical analysis. Statistical analyses [23, 24] of GNG13 expression were carried out using SPSS Statistics 20.0 (SPSS Inc., Chicago, IL, USA) and the Stata 12.0 (Stata Corp, College Station, TX, USA) software. We used χ^2 -tests for correlations

between GNG13 and EOC clinico-pathological factors. Multivariate Cox regression models were used to determine significant prognostic factors. Kaplan–Meier analysis and log-rank tests were used to evaluate OS. $p < 0.05$ was considered significant.

Bioinformatic analysis and Kaplan–Meier Plotter Curves. We used OncoPrint (https://www.oncoPrint.org), which is a database of RNA and DNA sequencing information intentioned by TCGA, the Gene Expression Omnibus and other literature to evaluate the expression of GNG13 in EOC tissues, using the search terms: “GNG13”, “Cancer vs. Normal Analysis,” Breast Cancer “Ovarian Cancer” and “mRNA” to obtain the expression data for EOC. These data were provided in the OncoPrint microarray database as the median center of log2. The Kaplan–Meier Plotter (http://kmplot.com/analysis/) was used to identify the correlation between GNG13 expression and OS in patients with EOC or BC.

Results

GNG13 expression in BC and EOC.

Analysis of the data deposited in the OncoPrint database indicated that the expression of GNG13 was significantly higher in BC and EOC than in normal tissues (Figures 1A, 1B). We next determined the levels of GNG13 mRNA in tissues in EOC and BC (Figures 2A, 2B). Western blot analysis was performed to detect GNG13 protein levels in EOC and BC (Figures 3A, 3B). Results showed that both mRNA and protein levels of GNG13 were higher in ovarian and breast cancer than in normal tissues.

GNG13 expression was greater in BC and EOC tissues. We used IHC to determine the GNG13 protein expression in the two cancers. GNG13 was positively stained in the cytoplasm of cancer cells. Typical GNG13 IHC staining patterns are presented in Figures 4A and 4B.

Relationship between GNG13 expression and clinical parameters of BC/EOC. In EOC, high GNG13 expression was significantly related to

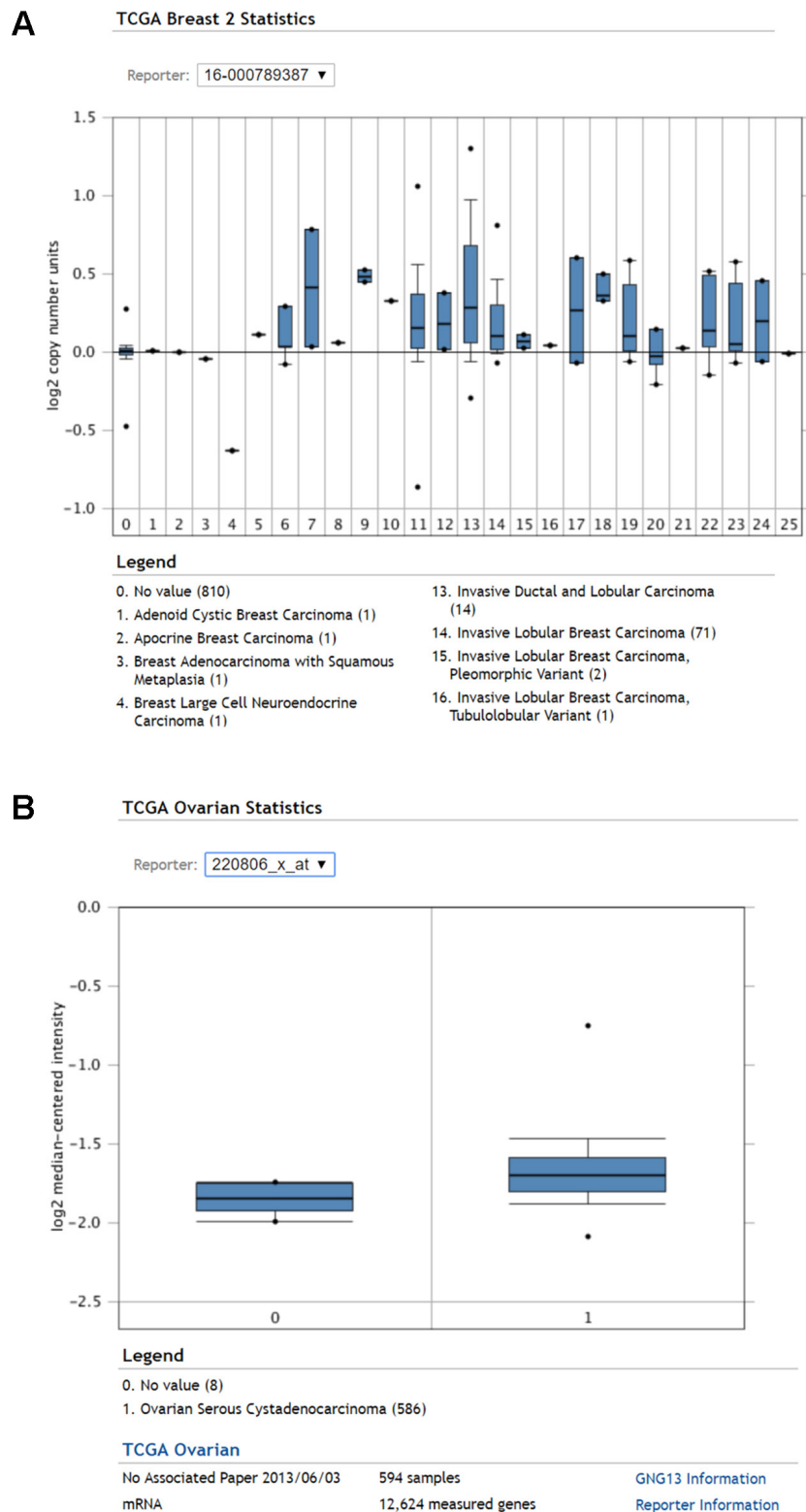


Figure 1. GNG13 mRNA is highly expressed in BC and EOC. OncoPrint database showed that different expression of GNG13 was found in BC tissues and adjacent normal tissue based on the TCGA (A). OncoPrint database was used to detect the expression of GNG13 in EOC by TCGA (B).

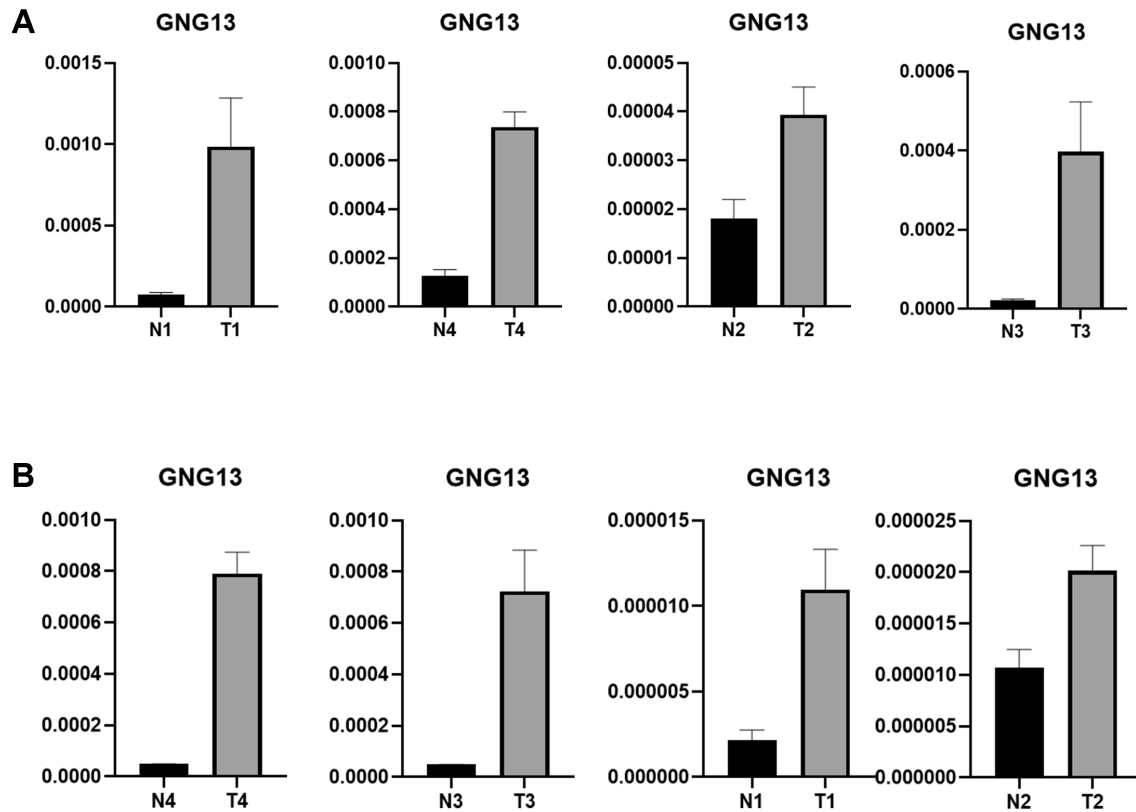


Figure 2. qRT-PCR assay was used to detect the GNG13 expression in BC (A) and EOC (B).

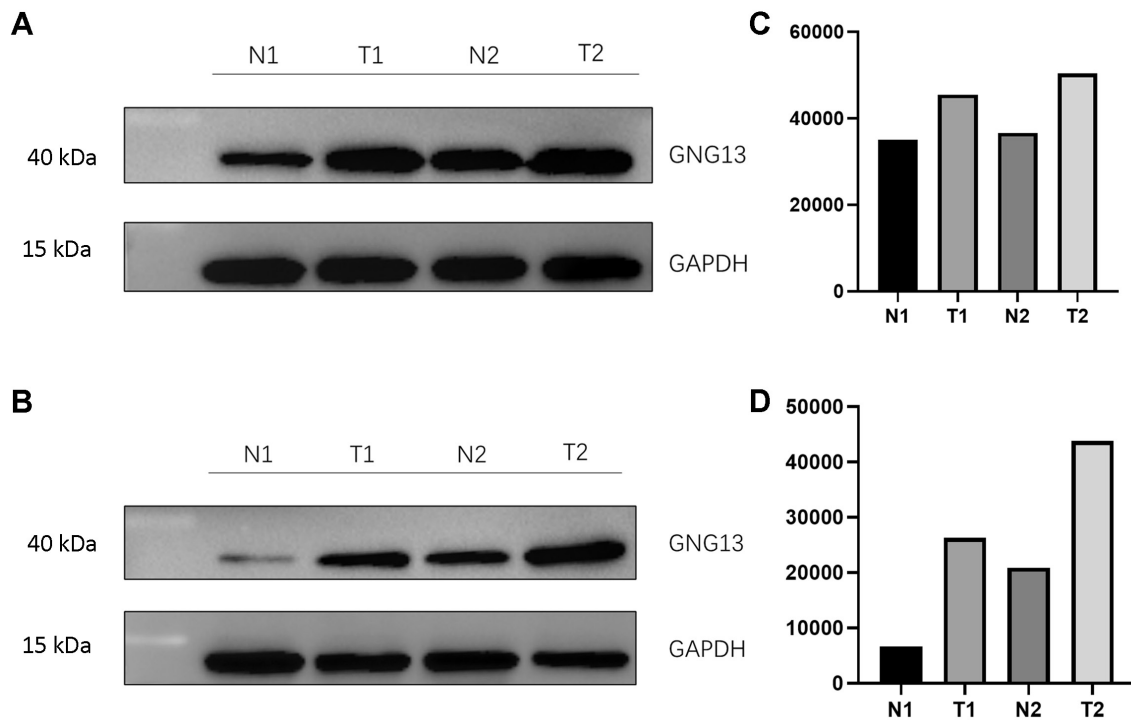


Figure 3. A) Western blot analysis of the expression of GNG13 in BC. B) Bar graph of the quantified data from A. C) Western blot analysis of the expression of GNG13 in EOC. D) Bar graph of the quantified data from C.

Table 1. Correlation of GNG13 expression with clinicopathological characteristics in ovarian cancer.

Groups	GNG13			Pearson χ^2	p-value
	n	Low or no	High		
Total	147	53 (36.05)	94 (63.94)		
Age				0.634	0.426
≤60 years	88	54 (61.36)	34 (38.64)		
>60 years	59	40 (67.80)	19 (36.20)		
FIGO stage				19.477	0.001*
1-2	63	53 (84.13)	10 (15.87)		
3-4	84	41 (48.81)	43 (51.19)		
Grade				7.609	0.006
Low grade	32	14 (43.75)	18 (56.25)		
High grade	114	80 (70.18)	34 (29.82)		
Histological classification				0.573	0.751
Serous carcinoma	111	73 (65.77)	38 (34.23)		
Endometrioid carcinoma	14	9 (64.29)	5 (35.71)		
Other ^a	21	12 (57.14)	9 (42.86)		
Lymph nodes				2.079	0.149
Yes	117	72 (61.54)	45 (38.46)		
No	29	22 (75.86)	7 (24.14)		
Metastasis				14.722	0.001*
Yes	83	42 (50.60)	41 (49.40)		
No	64	52 (81.25)	12 (18.75)		
Single or double				2.161	0.142
Single	94	56 (59.57)	38 (40.43)		
double	53	38(71.70)	15 (28.30)		
CA199				4.477	0.107
Yes	89	62 (69.66)	27 (30.34)		
No	20	13 (65.00)	7 (35.00)		
Unknow	38	19 (50.00)	19 (50.00)		
CA125				43.897	0.001*
≤100	29	4 (13.79)	25(86.21)		
>100	101	81 (80.20)	20 (19.80)		

Notes: *p<0.05 indicates a significant association among the variables; metastasis-pelvic lymph node metastases or nearby tissues and organs involved; ^aothers: clear cell carcinoma-5 cases; mucinous carcinoma-6 cases; transitional cell carcinoma-3 cases; adeno-squamous carcinoma-3 cases

Table 2. Correlation between the GNG13 expression and clinicopathological characteristics in breast cancer.

Characteristic	GNG13 expression (%)				Pearson χ^2	p-value
	n	Low or no	High			
Age (years)					1.184	0.553
≤40	11	4 (36.36)	7 (63.64)			
40-60	75	35 (46.67)	40 (53.33)			
≥60	39	21 (53.85)	18 (46.15)			
Tumor size (cm)					1.854	0.173
≤2 cm	60	25 (41.67)	35 (58.33)			
>2 cm	65	35 (53.85)	30 (46.15)			
Tumor grade					71.226	0.001*
I-II	55	3 (5.45)	52 (94.55)			
III	70	57 (81.43)	13 (18.57)			
ER					0.879	0.348
Negative	55	29 (52.73)	26 (47.27)			
Positive	70	31 (44.29)	39 (55.71)			
PR					0.006	0.939
Negative	85	41 (48.24)	44 (51.76)			
Positive	40	19 (47.50)	21 (52.50)			
HER-2 expression					0.045	0.832
Negative	99	48 (48.48)	51 (51.52)			
Positive	26	12 (46.15)	14 (53.85)			
Ki-67					1.418	0.234
Low	59	25 (6.74)	34 (93.26)			
High	66	35 (53.03)	31 (46.97)			
Molecular classification					2.729	0.142
Luminal A	38	14 (36.84)	24 (63.16)			
Luminal B	32	17 (53.13)	15 (46.88)			
Her2-overexpression	23	12 (52.17)	11 (47.83)			
TNBC	32	17 (53.13)	15 (46.88)			
N stage					4.477	0.107
N0	86	30 (34.88)	56 (65.12)			
N1+2+3	39	30 (76.92)	9 (23.08)			
TNM stage					18.066	0.001*
Stage I-II	58	16 (27.59)	42 (72.41)			
Stage III	67	44 (65.67)	23 (34.33)			

Note: *p<0.05 indicates a significant association among the variables

FIGO stage (p=0.001), presence of metastasis (p=0.001), and CA125 (p=0.001), but had no significant relationship to patients' age, tumor grade, histological classification, lymph node involvement, or CA199 expression (Table 1). In BC, high level of GNG13 expression was associated with tumor grade (p=0.001) and TNM stage (p=0.001). These data imply that EOC metastasis is related to GNG13 expression (Table 1 and Table 2).

Survival analysis. Univariate analysis showed that OS was associated with GNG13 expression (p<0.001), tumor grade (p=0.031), CA125 expression (p<0.001), lymph node involvement (p=0.002), metastasis (p<0.001), subtype (p=0.029), and FIGO stage (p<0.001) among patients with

EOC; and with GNG13 expression (p<0.001), histological grade (p<0.001), and TNM stage (p<0.001) among patients with BC (Table 3).

In multivariate analysis, OS was independently associated with GNG13 expression (hazard ratio [HR]: 0.259; p=0.003), FIGO stage ([HR]: 1.853; p=0.038), and age ([HR]: 1.815; p=0.013) among patients with EOC; and with GNG13 expression ([HR]: 0.292, p=0.014) and TNM stage ([HR]: 2.664, p=0.003) among patients with BC (Table 4).

Kaplan-Meier survival curves showed that both EOC patients and BC patients with low or no GNG13 expression had shorter OS than did their respective counterparts with high levels; and that patients with high FIGO stage

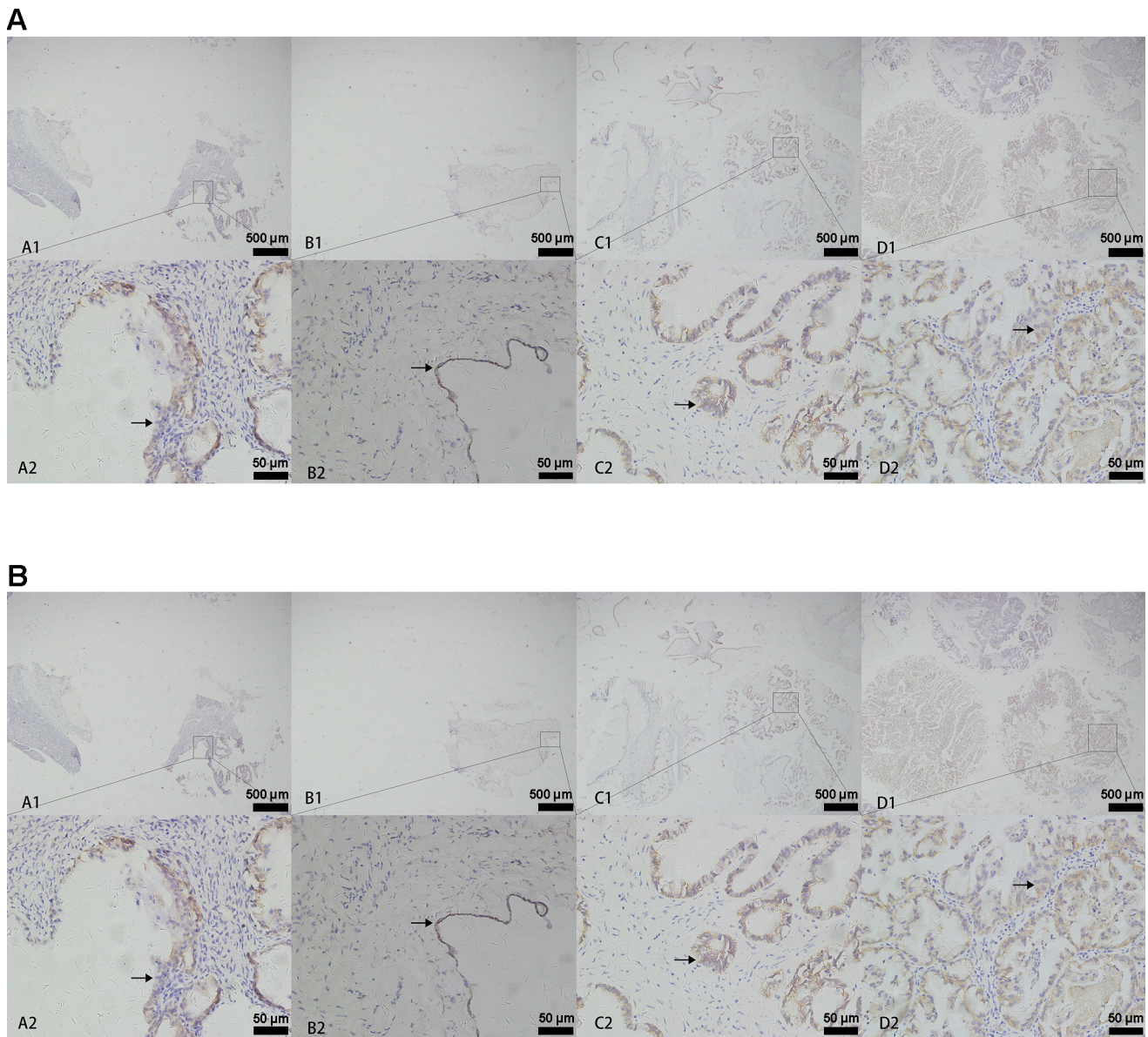


Figure 4. A) IHC analysis of GNG13 expression in BC (TMA). (A1) High IHC staining of GNG13 in the cytoplasm of the poorly differentiated invasive breast cancer cells. (B) High IHC staining of GNG13 in moderately differentiated invasive ductal carcinoma. (C) Low IHC staining of GNG13 in non-cancerous breast tissue cells. (D) Low IHC staining of GNG13 in the breast ductal papilloma cells. Original magnification 40× in (A–D); 400× in (A1–D1). B) GNG13 protein level in EOC tissues and normal and benign ovarian tissues by IHC. (A) Weak strong IHC staining of GNG13 in benign ovarian tumor. (B) Weak IHC staining of GNG13 in normal ovarian tissue. (C) Strong IHC staining of GNG13 in poorly differentiated EOC samples. (D) Strong IHC staining of GNG13 in highly differentiated EOC samples. Original magnification 40× in (A–D); 400× in (A1–D1).

EOC (Figures 5A–5C) and patients with TNM stage III BC (respectively) had shorter OS than patients with the lower-stage disease (Figures 5D, 5E).

Association between GNG13 expression and prognosis in Oncomine and Kaplan-Meier Plotter. To verify our finding of the relationship between OS and GNG13 expression in EOC and BC, we used Oncomine to analyze our data. The red column revealed the GNG13 mRNA upregulation. Consistent with our conclusions, GNG13 was lowly

expressed in both cancers compared with normal tissues (Figure 6). The Kaplan-Meier Plotter found that high GNG13 expression is a prognostic factor for OS ([HR]: 0.84; 95% CI: 0.75–0.94, $p=0.0017$; Figure 7).

Discussion

To our knowledge, this is the first study to use TMA-IHC and bioinformatics analysis to investigate correlations

Table 3. Univariate and multivariate Cox proportional hazard model analysis of prognostic markers for overall survival in ovarian cancer.

Variable	Univariate analysis			Multivariate analysis		
	HR	p-value	95% CI	HR	p-value	95% CI
GNG13 expression						
Low vs. High	0.219	0.001*	0.123–0.391	0.259	0.003*	0.105–0.637
Age (years)						
≤60 vs. >60	1.890	0.003*	1.236–2.890	1.815	0.013*	1.134–2.903
Grade						
Low vs. high	1.924	0.031*	1.062–3.486			
Single or double						
None vs. yes	1.460	0.090	0.942–2.262			
CA125						
None vs. yes	3.747	0.001*	1.711–8.205			
Lymph nodes						
None vs. yes	2.117	0.002*	1.314–3.411			
Metastasis						
None vs. yes	3.969	0.001*	2.515–6.263			
Type						
Serous vs. others	0.770	0.029*	0.609–0.974			
Ascites cell						
None vs. yes	1.608	0.153	0.839–3.082			
FIGO						
Stage I vs. stage II–IV	2.630	0.001*	1.788–3.867	1.853	0.038*	1.034–3.319

Note: *p<0.05; Abbreviations: Sc-serous carcinoma; Ec-endometrioid carcinoma; HR-Hazard ratio; CI-Confidence interval.

Table 4. Univariate and multivariate analysis of prognostic markers for overall survival in breast cancer.

Variable	Univariate analysis			Multivariate analysis		
	HR	p-value	95% CI	HR	p-value	95% CI
GNG13 expression						
High vs. low	0.161	0.001*	0.087–0.300	0.292	0.014*	0.110–0.777
Age (years)						
≤60 vs. >60	1.121	0.602	0.730–1.721			
ER expression						
Positive vs. negative	0.863	0.570	0.520–1.433			
PR expression						
Positive vs. negative	0.583	0.857	0.493–1.488			
Her2 expression						
Positive vs. negative	0.974	0.935	0.517–1.834			
Ki-67 expression						
Low vs. high	1.331	0.276	0.796–2.224			
Molecular classification						
Luminal A vs. luminal B vs. Her-2 overexpression vs. triple negative	1.090	0.435	0.878–1.352			
Histological grade						
I vs. II vs. III	4.391	0.001*	2.328–8.283	1.183	0.730	0.456–3.070
N stage						
N0 vs. N1+2+3	2.123	0.004	1.273–3.541	1.331	0.314	0.763–2.319
TNM stage						
Stage I–II vs. stage III	4.337	0.001*	2.338–8.046	2.664	0.004*	1.371–5.175

Note: *p<0.05; Abbreviations: ER-estrogen receptor; PR-progesterone receptor; T-tumor stage; N-lymph node metastasis stage; TNM-tumor-node metastasis; HR-hazard ratio; CI-confidence interval

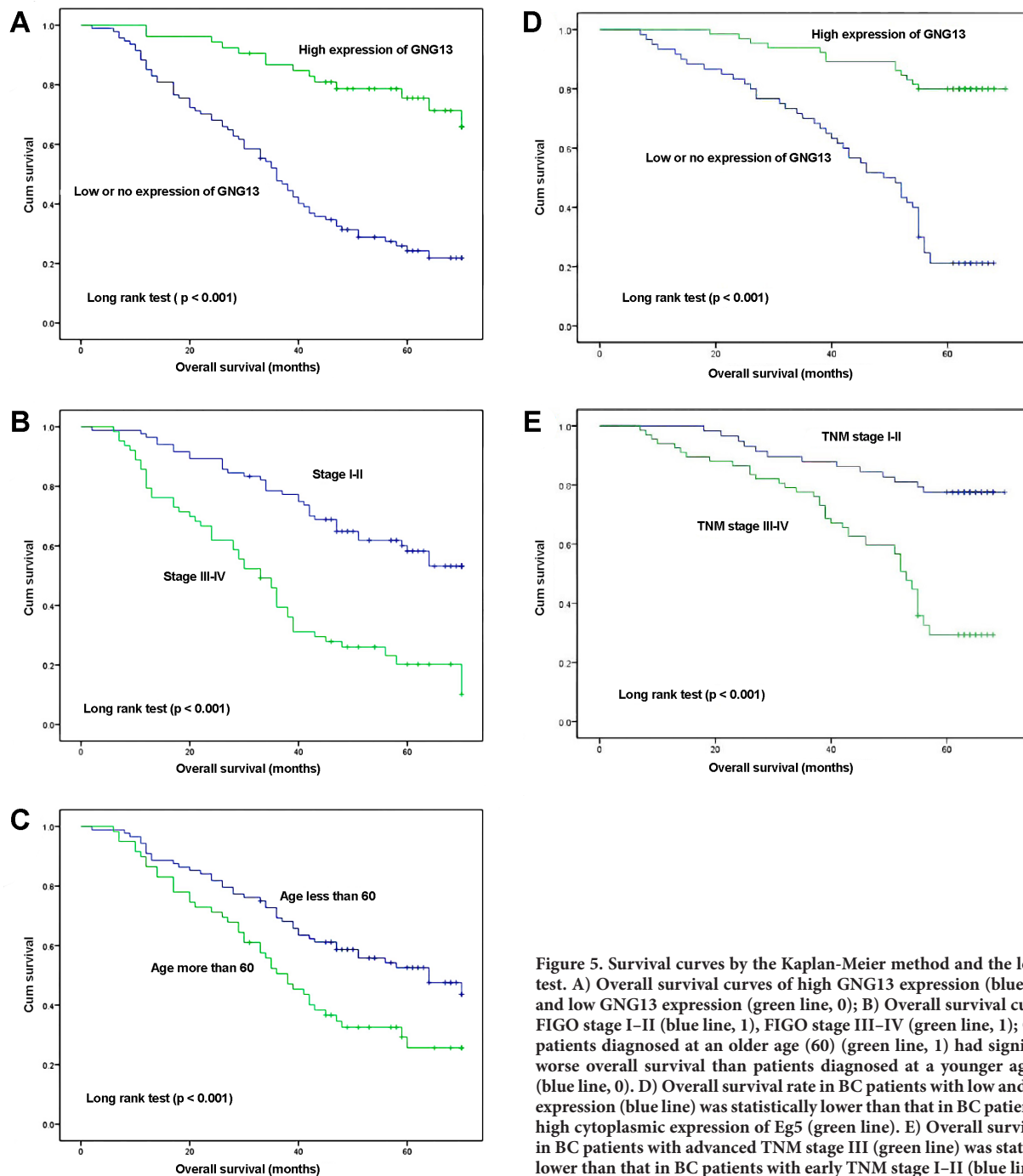


Figure 5. Survival curves by the Kaplan-Meier method and the log-rank test. A) Overall survival curves of high GNG13 expression (blue line, 1) and low GNG13 expression (green line, 0); B) Overall survival curves by FIGO stage I–II (blue line, 1), FIGO stage III–IV (green line, 1); C) EOC patients diagnosed at an older age (60) (green line, 1) had significantly worse overall survival than patients diagnosed at a younger age (<60) (blue line, 0). D) Overall survival rate in BC patients with low and no Eg5 expression (blue line) was statistically lower than that in BC patients with high cytoplasmic expression of Eg5 (green line). E) Overall survival rate in BC patients with advanced TNM stage III (green line) was statistically lower than that in BC patients with early TNM stage I–II (blue line).

between GNG13 protein levels and clinicopathological features of patients with EOC and BC. We detected that GNG13 protein expression in EOC and BC tissues is significantly lower than in non-cancerous tissues, while EOC and BC patients with high expression of GNG13 suffered a poor overall survival rate. To confirm our conclusions, the bioinformatics databases were used to identify relationships

between GNG13 expression and prognosis, which were consistent with our analysis.

GNG13 is part of a G-protein family that includes $G\alpha$, $G\beta$, and $G\gamma$ subunits [14]. It couples metabolic receptors and downstream effectors. GNG13 is essential for photoreactions in all retinas in bipolar cells and is involved in ovarian development [15]. Li et al. found that abnormal expression

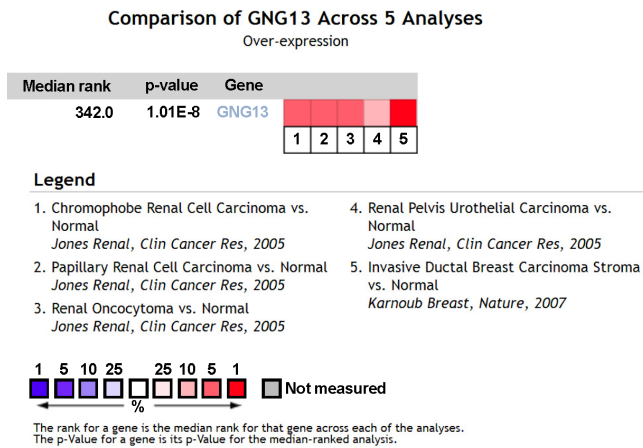


Figure 6. Two analyses were performed in comparing the RNA expression of GNG13 between cancer and normal tissue.

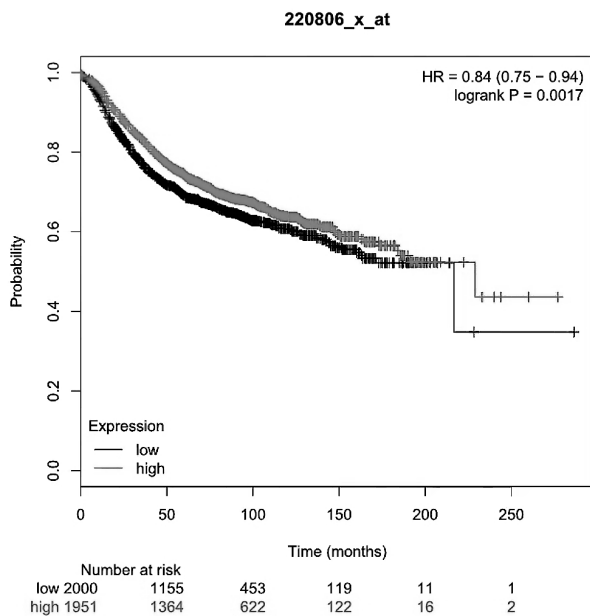


Figure 7. Prognostic value of GNG13 expression in Kaplan-Meier Plotter database. GNG13 probe number is 220806_x_at. 'Probability' on the y-axis represents the survival rates, the red line represents the patient with GNG13 expression above the median, the black line represents the patient with GNG13 expression below the median.

of GNG13 may lead to functional constipation and proposed a new idea to understand emotional disorders [25]. These results indicate that GNG13 has a relationship with ovary development; the bioinformatics databases confirmed our prediction. However, the role of GNG13 in the development and/or progression of cancer has not been reported, as far as we know. As structures and sequence domains cannot predict function, and prior knowledge of GNG13 is limited, determining the mechanism of a metastasis-suppressing mechanism is challenging.

Knowledge of BRCA1 and BRCA2 has opened new therapeutic opportunities through a wider understanding of breast and/or ovarian tumors [26]. Our results show that high GNG13 expression in BC and EOC specimens is significantly related to better survival. This biomarker could help predict prognosis and may be a metastasis suppressor in the two diseases. Therefore, our observations increase the understanding of the role of GNG13, especially in the development and progression of BC and EOC.

In conclusion, our study proved that abnormal expression of GNG13 may develop migration and invasive potential of EOC and BC and it could be used as a poor prognostic factor and potential therapeutic target for EOC and BC. However, our study has some limitations. First, it is retrospectively observational, and might not represent other BC and EOC populations. Second, more work should be done to identify the function of GNG13; a genome-wide shRNA screen *in vivo* and *in vitro* study might show whether GNG13 mediates metastasis. Further prospective study of this protein's mechanisms is needed to verify our findings.

Acknowledgments: National Natural Science Foundation of China, Grant/Award Number: 81802606.

References

- GLOSS B S, SAMIMI G. Epigenetic biomarkers in epithelial ovarian cancer. *Cancer Lett* 2014; 342: 257–263. <https://doi.org/10.1016/j.canlet.2011.12.036>
- SIEGEL R, MA J, ZOU Z, JEMAL A. Cancer statistics, 2014. *CA Cancer J Clin* 2014; 64: 9–29. <https://doi.org/10.3322/caac.21208>
- LIU J, MATULONIS UA. New strategies in ovarian cancer: translating the molecular complexity of ovarian cancer into treatment advances. *Clin Cancer Res* 2014; 20: 5150–5156. <https://doi.org/10.1158/1078-0432.CCR-14-1312>
- WALKER JL, POWELL CB, CHEN LM, CARTER J, BAE JUMP VL et al. Society of Gynecologic Oncology recommendations for the prevention of ovarian cancer. *Cancer* 2015; 121: 2108–2120.
- XU X, TANG X, LU M, TANG Q, ZHANG H et al. Over-expression of MAGE-A9 predicts unfavorable outcome in breast cancer. *Exp Mol Pathol* 2014; 97: 579–584. <https://doi.org/10.1016/j.yexmp.2014.11.001>
- PARKER JS, MULLINS M, CHEANG MCU, LEUNG S, VODUC D et al. Supervised risk predictor of breast cancer based on intrinsic subtypes. *J Clin Oncol* 2009; 27: 1160–1167. <https://doi.org/10.1200/JCO.2008.18.1370>
- CANCER GENOME ATLAS NETWORK. Comprehensive molecular portraits of human breast tumours. *Nature* 2012; 490: 61–70. <https://doi.org/10.1038/nature11412>
- LIN H, ZHANG H, WANG J, LU M, ZHENG F et al. A novel human Fab antibody for Trop2 inhibits breast cancer growth in vitro and in vivo. *Int J Cancer* 2014; 134: 1239–1249. <https://doi.org/10.1002/ijc.28451>

- [9] HUNN J, RODRIGUEZ GC. Ovarian cancer: etiology, risk factors, and epidemiology. *Clin Obstet Gynecol* 2012; 55: 3–23. <https://doi.org/10.1097/GRF.0b013e31824b4611>
- [10] BARNES DR, ANTONIOU AC. Unravelling modifiers of breast and ovarian cancer risk for BRCA1 and BRCA2 mutation carriers: update on genetic modifiers. *J Intern Med* 2012; 271: 331–343. <https://doi.org/10.1111/j.1365-2796.2011.02502.x>
- [11] HILLER DJ, CHU QD. Current Status of Poly(ADP-ribose) Polymerase Inhibitors as Novel Therapeutic Agents for Triple-Negative Breast Cancer. *Int J Breast Cancer* 2012; 2012: 829315. <https://doi.org/10.1155/2012/829315>
- [12] ZHONGQ, PENG HL, ZHAO X, ZHANG L, HWANG WT. Effects of BRCA1- and BRCA2-related mutations on ovarian and breast cancer survival: a meta-analysis. *Clin Cancer Res* 2015; 21: 211–220. <https://doi.org/10.1158/1078-0432.CCR-14-1816>
- [13] GANGI A, CASS I, PAIK D, BARMPPARAS G, KARLAN B et al. Breast cancer following ovarian cancer in BRCA mutation carriers. *JAMA Surg* 2014; 149: 1306–1313. <https://doi.org/10.1001/jamasurg.2014.1081>
- [14] KRISHNAN A, MUSTAFA A, ALMEN MS, FREDRIKSSON R, WILLIAMS MJ et al. Evolutionary hierarchy of vertebrate-like heterotrimeric G protein families. *Mol Phylogenet Evol* 2015; 91: 27–40. <https://doi.org/10.1016/j.ympev.2015.05.009>
- [15] ERICKSON RP, YATSENKO S, LARSON K, Cheung SW. A Case of Agonadism, Skeletal Malformations, Bicuspid Aortic Valve, and Delayed Development with a 16p13.3 Duplication Including GNG13 and SOX8 Upstream Enhancers: Are Either, Both or Neither Involved in the Phenotype? *Mol Syndromol* 2011; 1: 185–191. <https://doi.org/10.1159/000321957>
- [16] WALSTON ST, CHOW RH, WEILAND JD. Direct measurement of bipolar cell responses to electrical stimulation in wholemount mouse retina. *J Neural Eng* 2018; 15: 046003. <https://doi.org/10.1088/1741-2552/aab4ed>
- [17] FUJINO A, PIERETTI-VANMARCKE R, WONG A, DONAHOE PK, ARANGO NA. Sexual dimorphism of G-protein subunit Gng13 expression in the cortical region of the developing mouse ovary. *Dev Dyn* 2007; 236: 1991–1996. <https://doi.org/10.1002/dvdy.21183>
- [18] TUMMALA SR, NEINSTEIN A, FINA ME, DHINGRA A, VARDI N. Localization of Cacna1s to ON bipolar dendritic tips requires mGluR6-related cascade elements. *Invest Ophthalmol Vis Sci* 2014; 55: 1483–1492. <https://doi.org/10.1167/iops.13-13766>
- [19] EDGE SB, COMPTON CC. The American Joint Committee on Cancer: the 7th edition of the AJCC cancer staging manual and the future of TNM. *Ann Surg Oncol* 2010; 17: 1471–1474. <https://doi.org/10.1245/s10434-010-0985-4>
- [20] FENG Y, XUE WJ, LI P, SHA ZY, HUANG H et al. RASSF1A hypermethylation is associated with aflatoxin B1 and polycyclic aromatic hydrocarbon exposure in hepatocellular carcinoma. *Hepatogastroenterology* 2012; 59: 1883–1888. <https://doi.org/10.5754/hge11731>
- [21] LI F, PONISSERY-SAIDU S, YEE KK, WANG H, CHEN ML et al. Heterotrimeric G protein subunit Ggamma13 is critical to olfaction. *J Neurosci* 2013; 33: 7975–7984. <https://doi.org/10.1523/JNEUROSCI.5563-12.2013>
- [22] SUN R, WANG X, ZHU H, MEI H, WANG W et al. Prognostic value of LAMP3 and TP53 overexpression in benign and malignant gastrointestinal tissues. *Oncotarget* 2014; 5: 12398–12409. <https://doi.org/10.18632/oncotarget.2643>
- [23] HUANG J, ZHANG J, LI H, LU Z, SHAN W et al. VCAM1 expression correlated with tumorigenesis and poor prognosis in high grade serous ovarian cancer. *Am J Transl Res* 2013; 5: 336–346.
- [24] LI J, HUANG J, HUANG F, JIN Q, ZHU H et al. Decreased expression of IDH1-R132H correlates with poor survival in gastrointestinal cancer. *Oncotarget* 2016; 7: 73638–73650. <https://doi.org/10.18632/oncotarget.12039>
- [25] LI Y, SHI L, YUE L, GAO R, YU ZQ et al. Hippocampal gene expression profiling in a rat model of functional constipation reveals abnormal expression genes associated with cognitive function. *Neurosci Lett* 2018; 675: 103–109. <https://doi.org/10.1016/j.neulet.2018.03.023>
- [26] HOBERG-VETTI H, BJORVATN C, FIANE BE, AAS T, WOIE K et al. BRCA1/2 testing in newly diagnosed breast and ovarian cancer patients without prior genetic counseling: the DNA-BONus study. *Eur J Hum Genet* 2016; 24: 881–888. <https://doi.org/10.1038/ejhg.2015.196>